Enhanced Production of Low-Mass Electron Pairs in 200 GeV/Nucleon S-Au Collisions at the CERN Super Proton Synchrotron

G. Agakichiev,[1,*] R. Baur,[2] A. Breskin,[3] R. Chechik,[3] A. Drees,[2] C. Jacob,[1] U. Faschingbauer,[1] P. Fischer,[2] Z. Fraenkel,[3] Ch. Fuchs,[1] E. Gatti,[4] P. Glässel,[2] Th. Günzel,[2] C. P. de los Heros,[3] F. Hess,[1] D. Irmscher,[2] B. Lenkeit,[2] L. H. Olsen,[2] Y. Panebrattsev,[1,*] A. Pfeiffer,[2] I. Ravinovich,[3] P. Rehak,[5] A. Schön,[2] J. Schukraft,[6] M. Sampietro,[4] S. Shimansky,[6,*] A. Shor,[3] H. J. Specht,[2] V. Steiner,[3] S. Tapprogge,[2] G. Tel-Zur,[3] I. Tserruya,[3] Th. Ullrich,[2] J. P. Wurm,[1] and V. Yurevich[6,*]

(CERES Collaboration)

[1]*Max-Planck-Institut für Kernphysik, 69117 Heidelberg, Germany*
[2]*Physikalisches Institut der Universität Heidelberg, 69120 Heidelberg, Germany*
[3]*Weizmann Institute, Rehovot 76100, Israel*
[4]*Politecnico di Milano, 20133 Milano, Italy*
[5]*Brookhaven National Laboratory, Upton, New York 11973*
[6]*CERN, 1211 Geneva 23, Switzerland*

(Received 2 March 1995)

We report on measurements of low-mass electron pairs in 450 GeV p-Be, p-Au, and 200 GeV/nucleon S-Au collisions at central rapidities. For the proton induced interactions, the low-mass spectra are, within the systematic errors, satisfactorily explained by electron pairs from hadron decays, whereas in the S-Au system an enhancement over the hadronic contributions by a factor of $5.0 \pm 0.7(\text{stat}) \pm 2.0(\text{syst})$ in the invariant mass range $0.2 < m < 1.5$ GeV/c^2 is observed. The properties of the excess suggest that it arises from two-pion annihilation $\pi\pi \rightarrow e^+e^-$.

PACS numbers: 25.75.+r, 12.38.Mh, 13.85.Qk

Quantum chromodynamics predicts at very high densities and temperatures a phase transition from ordinary hadronic matter to a quark-gluon plasma, i.e., a state where quarks and gluons are not confined to hadrons. The energy densities achieved in fixed-target heavy ion collisions at the CERN Super Proton Synchrotron (SPS) are considered to be sufficiently high to reach such a phase transition. The ultimate motivation of the ongoing program is to put the conjectured plasma state to a stringent test and to learn about its properties.

The production of lepton pairs is commonly accepted as a promising probe to study the dynamical evolution of nuclear collision processes [1]. Leptons interact only electromagnetically, and their mean free path is considerably larger than the transverse size of the collision volume. They are produced during the entire space-time evolution of the system, beginning at the early hot stage up to the point where the hadrons cease to interact. Later, a large amount of additional lepton pairs is produced by the electromagnetic decays of hadronic particles. Since all stages of the collision have somewhat different contributions to the lepton spectrum, a careful analysis should, in principle, be able to unfold the whole space-time history of the hadronic collision, including contributions from both the quark (via $q\bar{q}$ annihilation) and the hadronic phase (via $\pi\pi$ annihilation) [2–5].

Up to now, two experiments have succeeded in measuring dimuons in heavy ion collisions at the CERN SPS, one at high masses [6], the other also in the low-mass range [7]. We present here the results of the first measurement of low-mass electron pairs in S-Au collisions taken with the CERES/NA45 spectrometer and compare them with those from p-Be and p-Au collisions obtained with the same apparatus. The systematic study from pp up to heavy nuclear systems is essential to identify any possible deviations from the mere superposition of pp collisions. We present here experimental evidence for such deviations, a strong enhancement of low-mass electron pairs in S-Au collisions.

CERES (Fig. 1) is an experiment dedicated to the measurement of low-mass electron pairs. The acceptance covers the pseudorapidity region $2.1 < \eta < 2.7$ and the invariant mass range from 50 MeV/c^2 to beyond 1 GeV/c^2. A detailed description of the CERES/NA45 experiment can be found in [8]. Here we summarize the most relevant features of the detector. Particle iden-

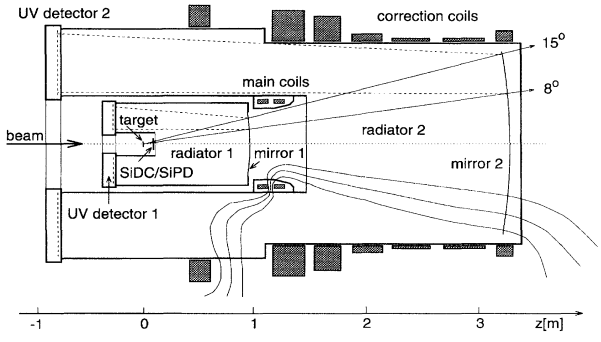

FIG. 1. Schematic view of the CERES spectrometer.

 0031-9007/95/75(7)/1272(4)$06.00

tification and directional tracking are based on two azimuthally symmetric RICH (ring imaging Cherenkov) detectors with a Cherenkov threshold ($\gamma_{\text{th}} \simeq 32$) high enough to substantially suppress signals from the large number of hadrons produced in the collision. A superconducting double solenoid between the two detectors provides an azimuthal deflection for momentum determination, leaving the polar angle θ unchanged. The magnetic field (sketched in Fig. 1) in the region of the inner RICH radiator is compensated to nearly zero using asymmetry in the currents of the coils, thus preserving the information of the original direction of the particles. A set of correction coils shapes the field in the second RICH radiator such that it points back to the target, ensuring straight trajectories and therefore sharp ring images. The Cherenkov photons from the RICH radiators are registered in two uv detectors, which are placed upstream of the target and are therefore not subject to the large flux of forward going charged particles. The information of the detectors is read out via two-dimensional arrays of about 50 000 pads each, allowing the unambiguous reconstruction of single photon hits.

A novel radial-drift silicon detector with 360 charge-collecting anodes on the outer perimeter of a 3-in. wafer [9] situated closely behind the target is used for high-resolution vertex reconstruction and tracking. Its prime purpose is to supply additional rejection of photon conversions and Dalitz pairs, which is necessary for a sufficient reduction of the combinatorial pair background in nucleus-nucleus collisions. An additional silicon pad detector [10] segmented into 64 pads supplies information about the charged-particle multiplicity for both first-level triggering and off-line analysis.

The S-Au results described in this Letter were obtained from the analysis of data taken during the SPS fixed-target running period in the spring of 1992. A total of 3.6×10^6 first-level and 2.7×10^6 second-level triggers were recorded. The first-level trigger uses the charged multiplicity information deduced from the silicon pad detector and was operated with two different thresholds in order to select events in a wide multiplicity range. One-half of the data sample covers the most central part of the total cross section (top 8% of $d\sigma/dn_{\text{ch}}$), whereas the other half contains semicentral events (top 38%) scaled down by a factor ~ 4, resulting in an average charged multiplicity of $\langle dn_{\text{ch}}/d\eta \rangle \simeq 125$ of the combined sample. The second-level trigger is formed by a systolic processor array [11] which searches for distant pairs of Cherenkov rings while suppressing the background of close pairs ($\theta_{ee} < 35$ mrad) from π^0 Dalitz decays and conversions. Since the original opening angle of the pairs is indispensable for this operation, only the data from the first RICH detector are used in the trigger.

The p-Be and p-Au data were taken in the summer of 1993. In addition to the setup for the sulfur beam, a fast intermediate-level trigger [8], based on a more restricted subsample of the inner RICH detector data, was used to further enhance the open pair signal, resulting in an overall enrichment factor of ~ 175 and ~ 75 for p-Be and p-Au, respectively. The data samples correspond to 2.1×10^9 minimum bias events in p-Be and 2.7×10^8 in p-Au collisions.

The off-line electron reconstruction is very similar in almost all aspects for p-Be, p-Au, and S-Au events. A pattern-recognition algorithm reconstructs ring images without the prior knowledge of the Cherenkov ring centers. Various ring quality criteria are applied to distinguish genuine Cherenkov rings from fake rings originating from random combinations of hits. For the S-Au data sample, these cuts are performed by a neural network algorithm in order to optimize the efficiency of the decision. The accepted rings in both RICH detectors are then combined to tracks, identified by their common angle θ with respect to the beam axis. Two tracks sharing the same unresolved double ring in the first RICH detector are rejected as photon conversion candidates. The remaining tracks are combined into pairs.

The combinatorial background originating from unrecognized partners of low-mass Dalitz and conversion pairs is *the* central problem of the experiment, and is the only significant source of physics background. Because the inclusive electron spectrum from π^0 Dalitz decays and conversions is considerably softer than that of pairs with $m > 0.2$ GeV/c^2, the signal-to-background ratio (S/B) can be significantly improved by a $p_\perp$ cut on the single electrons. The results discussed here are presented with a $p_\perp$ cut of 200 MeV/c for the S-Au data. Because of the lower background in proton induced collisions ($S/B \propto 1/n_{\text{ch}}$) a looser $p_\perp$ cut of 50 MeV/c has been chosen for the p-Be and p-Au samples. Further rejection cuts, most of them exploiting the small opening angle of the low-mass pairs, are applied to improve the S/B ratio. The most important are a close-ring cut in the first RICH to remove π^0 Dalitz and conversion pairs with unrecognized partners in the second RICH, a total ring-amplitude cut to reject unresolved double rings, and cuts on the match quality to the silicon drift chamber to eliminate conversions after the silicon detector and tracks not originating from the target. Although the S/B ratio in p-Be and p-Au collisions also improves with the use of the silicon drift detector, the pair signal itself decreases by a factor of 2 due to imperfections of the hardware; it was therefore not used in the analysis of the proton-nucleus data. In the S-Au data sample, however, its rejection power was essential due to the much smaller initial S/B ratio.

The combined effect of all cuts results in an improvement of the S/B ratio by 1 order of magnitude. In order to minimize the influence of the second-level trigger bias, only pairs with opening angles $\theta_{ee} > 35$ mrad are taken into account. The remaining combinatorial back-

ground in the e^+e^- sample is determined by the number of like-sign pairs. The pair signal S is then extracted by subtracting the like-sign contribution from the e^+e^- sample as $S = N_{+-} - 2(N_{++}N_{--})^{1/2}$.

The final S-Au sample for $m > 0.2$ GeV/c^2 consists of 4249 pairs, of which 2346 are e^+e^-, resulting in a net pair signal of 445 ± 65 with a S/B ratio of 1/4.3, while in the high-statistics p-Be (p-Au) sample a signal of 5760 ± 184 (1126 ± 100) pairs is obtained at a S/B ratio of 1/2.2 (1/4.5).

In the absence of *new* physics, the expected sources of electron pairs are hadron decays. For pair masses below 140 MeV/c^2, the π^0 Dalitz decay dominates the spectrum, whereas at higher masses the decays $\eta \rightarrow e^+e^-\gamma$, $\omega \rightarrow e^+e^-\pi^0$, and $\rho/\omega \rightarrow e^+e^-$ should be the most significant. We have calculated the invariant-mass spectrum with a generator containing all known hadronic sources, i.e., the π^0, η, η', ρ, ω, and ϕ. The particle ratios of these "conventional" sources are assumed to be independent of the collision system and to scale with the number of produced particles. Their $p_\perp$ distributions were generated assuming $m_\perp$ scaling [12] based on pion $p_\perp$ spectra from different experiments [13–15]. The rapidity distribution for pions was a fit to measured data [16] for S-Au, which was modified for the heavier mesons to reflect the respective ratio of $\sigma_{\text{central}}/\sigma_{\text{tot}}$ as measured by NA27 [17] for pp; the relative rapidity densities for the various mesons were also taken from Ref. [17]. All Dalitz decays were treated according to the Kroll-Wada expression with the experimental transition form factors taken from Ref. [18]; the vector meson decays were generated using the expressions derived by Gounaris and Sakurai in Ref. [19]. Charm production was not taken into account, since it is negligible in the low-mass range. Finally, the laboratory momenta of the electrons were convoluted with the experimental resolution and acceptance.

The results for the p-Be, p-Au, and S-Au data samples are shown in Figs. 2, 3, and 4. All three spectra are normalized to represent *pair density per charged-particle density* within the rapidity acceptance $2.1 < y < 2.65$; the average charged-particle densities used in the normalization are quoted in the figures. The data are corrected for trigger enrichment and for pair reconstruction efficiency. For proton-induced reactions, the pair reconstruction efficiency is about 50%. In the S-Au analysis, more stringent cuts, including cuts on the silicon drift detector information, were necessary to sufficiently reduce the combinatorial background. The reconstruction efficiency is 17% for $dn_{\text{ch}}/dy = 50$, decreasing to 7% for $dn_{\text{ch}}/dy = 200$. It is rather uniform in mass, but drops by 40% for masses below 150 MeV/c^2. The systematic uncertainties on the e^+e^- yield are approximately equal for all observed collision systems and amount to ±25% for the trigger enrichment and ±30% for the pair reconstruction efficiency. In the figures, the statistical errors are marked by bars, whereas the brackets reflect the systematic uncertainties linearly added to the statistical errors. The data are *not* corrected for pair acceptance (i.e., the ratio of the geometrical acceptances of the virtual photon to the two tracks of the pair), since this correction would require deeper knowledge of all sources of pairs, which obviously does not yet exist for the S-Au case. For pairs emerging from hadron decays the pair acceptance is ~0.14 in the ρ/ω mass region and increases to unity towards mass zero.

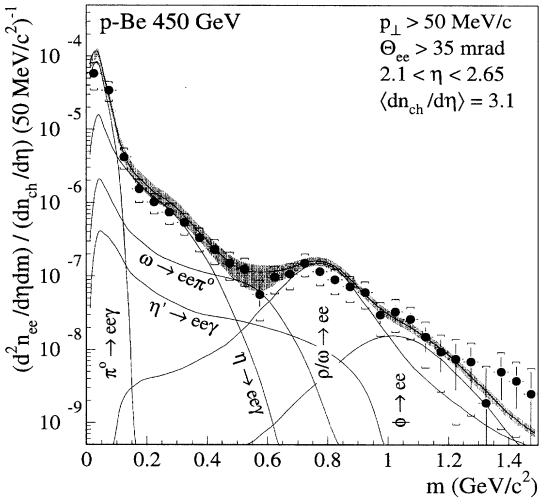

FIG. 2. Inclusive e^+e^- mass spectra in 450 GeV p-Be collisions showing the data (full circles) and the various contributions from hadron decays. The shaded region indicates the systematic error on the summed contributions. No pair-acceptance corrections are applied.

The various contributions from hadron decays for the respective colliding systems are shown in all three figures.

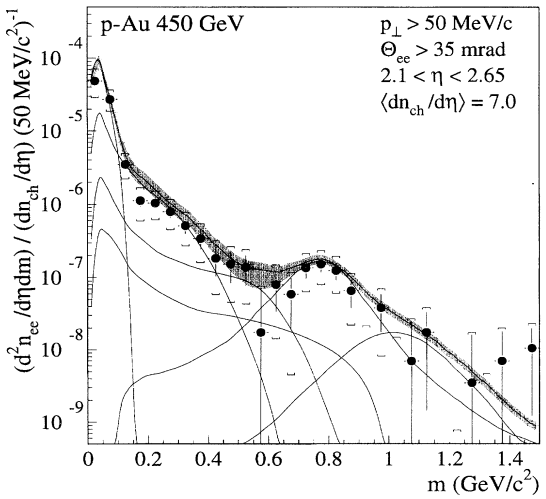

FIG. 3. Inclusive e^+e^- mass spectra in 450 GeV p-Au collisions. For explanations see Fig. 2.

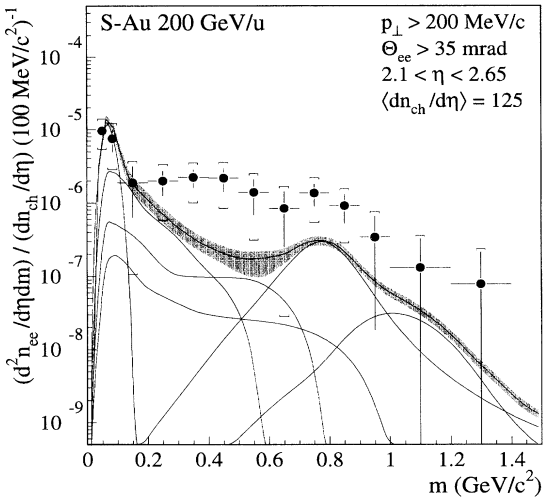

FIG. 4. Inclusive e^+e^- mass spectra in 200 GeV/nucleon S-Au collisions. For explanations see Fig. 2.

The shaded region indicates the systematic error on the total contribution from hadron decays; it varies with mass between 12% and 45%, due to large uncertainties in the branching ratios and/or electromagnetic form factors for the various meson decays. In order to allow for a meaningful comparison, the calculations are subject to the same filters as the data, namely, pair acceptance, $p_\perp$ cut, and opening-angle cut.

The measured inclusive e^+e^--pair spectrum in p-Be is well explained, within the present systematic errors, by electron pairs from hadron decays, and there is no need to invoke any unconventional source as also reported previously in Ref. [20]. The same conclusion holds in p-Au collisions, and this is a new and interesting result in itself. In the S-Au data sample, however, a statistically significant enhancement is observed. As a quantitative measure of the observed excess we define the enhancement factor as the integral of the data over the integral of the predicted sources in the mass range $0.2 < m < 1.5$ GeV/c^2, which results in $5.0 \pm 0.7(\text{stat}) \pm 2.0(\text{syst})$. A striking feature of the S-Au spectrum is the absence of any enhancement for masses below approximately 250 MeV/c^2. A second independent analysis gives essentially the same results [21].

If the observed excess originates from collective processes in a thermalized system, it should vary as the square of the charged-particle density. Although quantitative studies of this characteristic behavior suffer from the limited statistics of our S-Au data sample, one can derive an indication of a quadratic dependence by comparing our data with results obtained by the HELIOS/3 Collaboration, also reporting an excess production of dileptons in the low-mass region. The HELIOS/3 Collaboration has measured dimuon production in 200 GeV/nucleon S-W collisions and 200 GeV p-W collisions at more forward rapidities $y > 3.5$ [7]. The observed $\mu^+\mu^-$ spectrum shows a similar onset of the excess around $m_{\mu\mu} \approx 2m_\pi$. However, the magnitude of the enhancement factor—which we have derived from their data as the integral of the S-W data over the integral of the p-W data in the comparable mass range—is significantly smaller ($\simeq 1.6$). This difference could be explained by a nonlinear dependence of the underlying production mechanism. Indeed, the average charged-particle densities accessible by the two experiments, and hence the energy densities, differ by at least a factor of 2 (due to the more central rapidity coverage of the CERES experiment). This, taken together with the onset of the excess at $m_{ee} \simeq 2m_\pi$ and the persistence of the enhancement in the ρ region, suggests that we observe two-pion annihilation $\pi\pi \rightarrow e^+e^-$.

The CERES Collaboration acknowledges the good performance of the CERN PS and SPS accelerators. We are grateful for support by the German Bundesministerium für Forschung und Technologie under Grant BMFT 06HD525I, the U.S. Department of Energy under Contract No. DE-AC02-76CH00016, the MINERVA Foundation, Munich/Germany, the H. Gutwirth Fund, and the Israeli Science Foundation.

*Visiting from JINR, Dubna, Russia.

[1] E. V. Shuryak, Phys. Lett. **78B**, 150 (1978).
[2] K. Kajantie *et al.*, Phys. Rev. D **34**, 2746 (1986).
[3] P. V. Ruuskanen, Nucl. Phys. **A544**, 169c (1992).
[4] J. Cleymans, V. V. Goloviznin, and K. Redlich, Z. Phys. C **59**, 495 (1993).
[5] P. Koch, Z. Phys. C **57**, 283 (1993).
[6] M. C. Abreu *et al.*, Nucl. Phys. **A566**, 77c (1994).
[7] M. Masera, in Proceedings of the Eleventh International Conference on Ultra-Relativistic Nucleus-Nucleus Collisions, Monterey, 1995 (to be published).
[8] R. Baur *et al.*, Nucl. Instrum. Methods Phys. Res., Sect. A **343**, 87 (1994).
[9] W. Chen *et al.*, IEEE Trans. Nucl. Sci. **39**, 619 (1992).
[10] T. F. Günzel *et al.*, Nucl. Instrum. Methods Phys. Res., Sect. A **316**, 259 (1992).
[11] J. Gläß *et al.*, IEEE Trans. Nucl. Sci. **37**, 241 (1990).
[12] M. Bourquin and J. M. Gaillard, Nucl. Phys. **B114**, 334 (1976).
[13] T. Åkesson *et al.*, Z. Phys. C **46**, 361 (1992).
[14] T. Alber *et al.*, Nucl. Phys. **A566**, 35c (1994).
[15] R. Santo *et al.*, Nucl. Phys. **A566**, 61c (1994).
[16] R. Albrecht *et al.*, Z. Phys. C **55**, 539 (1992).
[17] M. Aguilar-Benitez *et al.*, Z. Phys. C **50**, 405 (1991).
[18] L. G. Landsberg, Phys. Rep. **128**, 301 (1985).
[19] G. J. Gounaris and J. J. Sakurai, Phys. Rev. Lett. **21**, 244 (1968).
[20] T. Åkesson *et al.*, Z. Phys. C (to be published).
[21] C. P. de los Heros, Weizmann Institute of Science, Ph.D. thesis (to be published).